

Levitation of a metallic sphere near gas-liquid and liquid-liquid interfaces by the repulsive Casimir force

Norio Inui*

Graduate School of Engineering, University of Hyogo, Shosha 2167, Himeji, Hyogo 671-2201, Japan

(Received 26 March 2014; published 12 June 2014)

By counteracting gravity, the repulsive Casimir force enables stable levitation of a perfectly conducting particle near a liquid-air interface if the particle exists inside the liquid. In the present study, we examine the levitation of a gold particle near a bromobenzene-air interface and calculate the levitation height using the scattering-matrix formulation. In addition, we consider the Casimir force acting on a gold sphere near the interface between bromobenzene and water. At asymptotically large separations, the Casimir force is attractive because of the large static dielectric permittivity of water. However, the Casimir force changes from attractive to repulsive as the separation decreases. We also found that the gold particle can be levitated in bromobenzene above water.

DOI: [10.1103/PhysRevA.89.062506](https://doi.org/10.1103/PhysRevA.89.062506)

PACS number(s): 31.30.jh, 34.35.+a, 68.03.-g, 68.05.-n

I. INTRODUCTION

Advancements in the study of the Casimir effect [1,2] have led to many promising applications in nanotechnology, including the levitation of nanoparticles using the repulsive Casimir force [3–15]. Mundy *et al.* have experimentally shown that the Casimir force between a gold sphere and a silica plate immersed in bromobenzene (C_6H_5Br) can be repulsive [16–18]. However, levitation using the repulsive Casimir force, which is termed quantum levitation, has not yet been applied to nanotechnology. To broaden the scope of applications for quantum levitation, this study provides numerical results showing that quantum levitation may be realized near not only liquid-solid interfaces but also gas-liquid and liquid-liquid interfaces.

To generate the repulsive Casimir force, the order of the dielectric permittivity along the relevant materials' imaginary frequency $\epsilon(i\xi)$ is an important factor. When a particle with permittivity $\epsilon_1(i\xi)$ is immersed in a liquid with permittivity $\epsilon_3(i\xi)$ above a flat medium with permittivity $\epsilon_2(i\xi)$, the Casimir force between the particle and the flat medium can be repulsive if the inequality $\epsilon_2(i\xi) < \epsilon_3(i\xi) < \epsilon_1(i\xi)$ holds for any frequency of the electromagnetic field. The minimum value of $\epsilon(i\xi)$ is 1, and the dielectric permittivity of air is very close to 1. It follows from this condition that almost all metallic particles with sufficiently small radii can be levitated near a liquid-air interface by the repulsive Casimir force.

The above inequality is not a necessary and sufficient condition for quantum levitation by the repulsive Casimir force. Even if the inequality does not hold over a limited frequency interval, the Casimir force can be repulsive for a limited separation interval. For example, the dielectric permittivity of water is much larger than the dielectric permittivity of bromobenzene near low frequencies. Therefore, when a particle is immersed in bromobenzene, the inequality is not satisfied for low frequencies. However, the Casimir force can be repulsive if the particle is located near to the water-bromobenzene interface.

The levitation height is a crucial factor when applying the quantum levitation of a nanoparticle to nanotechnology. If the distance between the particle and the interface is much

smaller than the radius of the particle, the proximity force approximation (PFA) provides a good approximate levitation height. However, if the levitation height is comparable to or larger than the radius of the particle, the PFA is not suitable. During the past decade, there has been rapid progress in the computation of the Casimir force between a sphere and a plate, and this progress has enabled us to calculate the levitation height of small particles.

The stability of the levitation is also an important consideration. Because of bombardment by surrounding molecules [19], the particle position in a liquid is always fluctuating about its equilibrium position. In particular, because the particle is often more stable at the liquid-liquid interface than at the equilibrium position where the repulsive Casimir force balances gravity, we must compare the Casimir energy with the surface tension at the liquid-liquid interface.

The remainder of this paper is structured as follows. In Sec. II, we introduce the PFA and scattering-matrix formulation [20–23], and we consider the asymptotic behavior of the Casimir force between a neutral metallic sphere and a plate at both small and large separations. In Sec. III, we calculate the Casimir force acting on gold particles of 100 and 500 nm radii near an interface between bromobenzene and air, and we then discuss the levitation height. In Sec. IV, we consider the quantum levitation of a gold particle above water. In particular, we focus on the change in the direction of the Casimir force as the separation increases. The dielectrophoretic force resulting from the surface potential at the bromobenzene-water interface is also considered. In Sec. V, we present our conclusions and discuss the possibility of the directly measuring quantum levitation [24].

II. THE CASIMIR ENERGY OF A LEVITATED METALLIC SPHERE

A. The Casimir energy at asymptotically small separations

We consider the Casimir energy of a sphere with radius R and dielectric permittivity $\epsilon^{(1)}(\xi)$ placed in a medium with dielectric permittivity $\epsilon^{(3)}(\xi)$, which is in contact with a flat medium with dielectric permittivity $\epsilon^{(2)}(\xi)$ (as shown in Fig. 1). If the distance a between the gold particle and the flat medium is much smaller than the particle radius, the Casimir force can

*inui@eng.u-hyogo.ac.jp

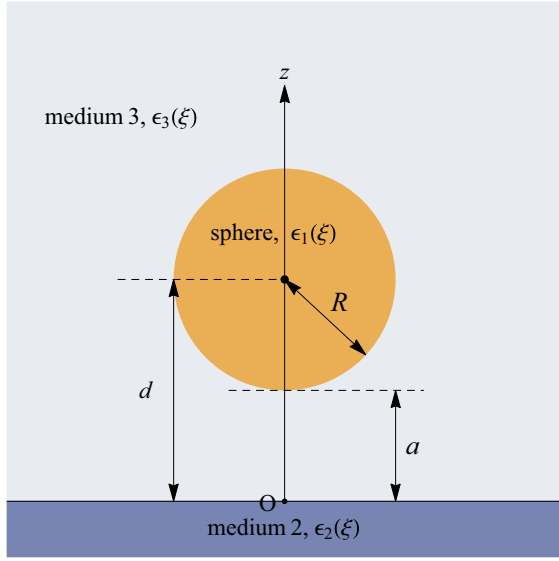


FIG. 1. (Color online) Schematic of the materials used for levitation by the repulsive Casimir force.

be calculated using the PFA, as follows [1]:

$$F(a) = 2\pi R E_{\text{pp}}(a), \quad (1)$$

where $E_{\text{pp}}(a)$ is the Casimir energy per unit area in the parallel configuration of a gold plate and a flat medium with gap a .

The Casimir energy between two plates with dielectric permittivities $\epsilon^{(1)}(\xi)$ and $\epsilon^{(2)}(\xi)$, which are separated by a medium with permittivity $\epsilon^{(3)}(\xi)$ at temperature T , is given by the well-known Lifshitz formula [25]:

$$E_{\text{pp}}(a) = \frac{k_B T}{2\pi} \sum_{l=0}^{\infty}{}' \int_0^{\infty} k_{\perp} dk_{\perp} \{G_{\text{TM}}(\xi_l, k_{\perp}) + G_{\text{TE}}(\xi_l, k_{\perp})\}, \quad (2)$$

where k_B is the Boltzmann constant, and k_{\perp} is the modulus of the projection of the light wave vector on the plate. The summation is performed over the Matsubara frequency, which is given by $\xi_l = 2\pi k_B T l / \hbar$. The prime symbol near the summation sign indicates the multiples of the term containing $l = 0$ by a factor of 1/2. Functions G_{TM} and G_{TE} in Eq. (2) are characterized by two independent polarizations: transverse magnetic (TM) and transverse electric (TE) modes. They are defined as

$$G_{\text{TM}}(\xi_l, k_{\perp}) = \ln \left[1 - r_{\text{TM}}^{(1)} r_{\text{TM}}^{(2)}(i\xi_l, k_{\perp}) e^{-2k_l^{(3)} a} \right],$$

$$G_{\text{TE}}(\xi_l, k_{\perp}) = \ln \left[1 - r_{\text{TE}}^{(1)} r_{\text{TE}}^{(2)}(i\xi_l, k_{\perp}) e^{-2k_l^{(3)} a} \right],$$

where $k_l^{(n)} \equiv k_l^{(n)}(i\xi_l, k_{\perp}) = \sqrt{k_{\perp}^2 + \epsilon^{(n)}(i\xi_l) \xi_l^2 / c^2}$. In the above equations, the reflection coefficients for the TM and TE modes are given by

$$r_{\text{TM}}^{(n)}(i\xi_l, k_{\perp}) = \frac{\epsilon_l^{(n)} k_l^{(3)} - \epsilon_l^{(3)} k_l^{(n)}}{\epsilon_l^{(3)} k_l^{(n)} + \epsilon_l^{(n)} k_l^{(3)}}, \quad (3)$$

$$r_{\text{TE}}^{(n)}(i\xi_l, k_{\perp}) = \frac{k_l^{(3)} - k_l^{(n)}}{k_l^{(3)} + k_l^{(n)}}, \quad (4)$$

where $\epsilon_l^{(n)} = \epsilon^{(n)}(i\xi_l)$ is the dielectric permittivity along the imaginary frequency.

At absolute zero, Eq. (2) is replaced with

$$E_{\text{pp}}^{\text{zero}}(a) = \frac{\hbar}{4\pi^2} \int_0^{\infty} k_{\perp} dk_{\perp} \int_0^{\infty} d\xi \{G_{\text{TM}}(\xi, k_{\perp}) + G_{\text{TE}}(\xi_l, k_{\perp})\}. \quad (5)$$

Introducing a new variable $p \equiv \sqrt{1 + c^2 k^2 / [\epsilon^{(3)}(i\xi) \xi^2]}$, the Casimir energy $E_{\text{pp}}^{\text{zero}}(a)$ is written as

$$E_{\text{pp}}^{\text{zero}}(a) = \frac{\hbar}{4\pi^2 c^2} \int_1^{\infty} p dp \int_0^{\infty} \epsilon^{(3)}(i\xi) \xi^2 d\xi \times \left\{ \ln \left[1 - \frac{\epsilon^{(1)} p - \epsilon^{(3)} s_1}{\epsilon^{(1)} p + \epsilon^{(3)} s_1} \frac{\epsilon^{(2)} p - \epsilon^{(3)} s_2}{\epsilon^{(1)} p + \epsilon^{(3)} s_2} e^{-2\xi p \sqrt{\epsilon^{(3)} a / c}} \right] + \ln \left[1 - \frac{p - s_1}{p + s_1} \frac{p - s_2}{p + s_2} e^{-2\xi p \sqrt{\epsilon^{(3)} a / c}} \right] \right\}, \quad (6)$$

where $s_j \equiv \sqrt{p^2 - 1 + \epsilon^{(j)}(i\xi) / \epsilon^{(3)}(i\xi)}$. At small separations, the dominant contribution is from $p \gg 1$. Thus, if $p \approx s_1$ and $p \approx s_2$, the contribution from the TE mode is much smaller than that of the TM mode, and the Casimir energy can be approximated by

$$E_{\text{pp}}^{\text{zero}}(a) \approx -\frac{\hbar}{16\pi^2 a^2} \int_0^{\infty} d\xi \text{Li}_3 \left[\frac{\epsilon^{(1)} - \epsilon^{(3)}}{\epsilon^{(1)} + \epsilon^{(3)}} \frac{\epsilon^{(2)} - \epsilon^{(3)}}{\epsilon^{(2)} + \epsilon^{(3)}} \right], \quad (7)$$

where $\text{Li}_3(x)$ is the polylogarithm of order 3. Because the thermal correction is not significant for small separations, the Casimir force between a sphere and a flat medium is proportional to the radius and inversely proportional to the square of the separation for small separations. Combining the PFA and Eq. (7), we derive the Casimir force at small separations:

$$F_{\text{sp}}(a) \approx -\frac{\hbar R}{8\pi a^2} \int_0^{\infty} d\xi \text{Li}_3 \left[\frac{\epsilon^{(1)} - \epsilon^{(3)}}{\epsilon^{(1)} + \epsilon^{(3)}} \frac{\epsilon^{(2)} - \epsilon^{(3)}}{\epsilon^{(2)} + \epsilon^{(3)}} \right], \quad (8)$$

$$a \ll R.$$

B. The Casimir energy for asymptotically large separations

To obtain the Casimir energy for large separations, we employ the scattering-matrix formulation; in particular, we use the expression given by Zandi *et al.* (more details are given in Ref. [22]). At zero temperature, the Casimir energy between a sphere and a flat medium is given by

$$E_{\text{sp}}^{\text{zero}}(d) = \sum_{m=0}^{\infty}{}' E_m(d), \quad (9)$$

$$E_m(d) = \frac{\hbar c}{\pi} \int_0^{\infty} d\kappa \ln \det [I - R_m(\kappa)], \quad (10)$$

where $d = a + R$, κ is the wave number of the electromagnetic field, and m denotes the angular momentum eigenvalue that characterizes the reflection on the sphere [23]. Matrix R_m is

defined by

$$R_m = \begin{pmatrix} R_m^{EE} & R_m^{EM} \\ R_m^{ME} & R_m^{MM} \end{pmatrix}. \quad (11)$$

Here, the entry in the i th row and j th column of block matrix $R_m^{\alpha\beta}$ is given by the product of the propagation and scattering operator for sphere R_s^α and for flat medium R_f^α as

$$[R_m^{\alpha\beta}]_{ij} = R_{s,l}^\alpha R_{f,l'm}^{\alpha\beta}, \quad (12)$$

where $l = i + m - 1 + \delta_{m0}$ and $l' = j + m - 1 + \delta_{m0}$. The scattering operator for the sphere $R_s^{\alpha\beta}$ can be written in terms of Mie coefficients using modified Bessel functions $I_{l+1/2}(z)$ and $K_{l+1/2}(z)$:

$$R_{s,l}^M = \frac{\pi}{2} \frac{I_{l+1/2}(\tilde{\kappa})\hat{I}_{l+1/2}(n\tilde{\kappa}) - I_{l+1/2}(n\tilde{\kappa})\hat{I}_{l+1/2}(\tilde{\kappa})}{K_{l+1/2}(\tilde{\kappa})\hat{I}_{l+1/2}(n\tilde{\kappa}) - I_{l+1/2}(n\tilde{\kappa})\hat{K}_{l+1/2}(\tilde{\kappa})}, \quad (13)$$

$$R_{s,l}^E = -\frac{\pi}{2} \frac{I_{l+1/2}(\tilde{\kappa})\hat{I}_{l+1/2}(n\tilde{\kappa}) - n^2 I_{l+1/2}(n\tilde{\kappa})\hat{I}_{l+1/2}(\tilde{\kappa})}{K_{l+1/2}(\tilde{\kappa})\hat{I}_{l+1/2}(n\tilde{\kappa}) - n^2 I_{l+1/2}(n\tilde{\kappa})\hat{K}_{l+1/2}(\tilde{\kappa})}, \quad (14)$$

$$\hat{I}_l(z) \equiv I_l(z) + 2zI'_l(z), \quad (15)$$

$$\hat{K}_l(z) \equiv K_l(z) + 2zK'_l(z), \quad (16)$$

where $\tilde{\kappa} = \kappa R$ and $n = \sqrt{\epsilon_1(i\xi)/\epsilon_3(i\xi)}$. The elements of $R_{f,l'm}^\alpha$ describing the propagation of waves between the plate and the sphere are given by

$$R_{f,l'm}^{\alpha\beta} = \int_0^\infty \frac{zdz}{4\pi} \frac{e^{-2d\kappa\sqrt{1+z^2}}}{\sqrt{1+z^2}} \sum_{\gamma \in \{M,E\}} D_{lm}^{\alpha\gamma}(z) r_p^\gamma(\kappa, z) D_{l'm}^{\beta\gamma^*}(z), \quad (17)$$

where $z = \sqrt{\epsilon_3(i\xi)\xi^2/c^2 + \kappa^2}/\kappa$ and $r_p^\gamma(\kappa, z)$ is defined by replacing ξ_l in $r_\gamma^{(2)}(i\xi_l, k_\perp)$ [see Eqs. (3) and (4)] with $c\kappa$. Matrices $D_{lm}^{\alpha\gamma}$ in Eq. (17) decompose a multiple wave into plane waves and are defined as

$$D_{lm}^{MM} = D_{lm}^{EE} = \sqrt{\frac{4\pi(2l+1)(l-m)!}{l(l+1)(l+m)!}} z \left. \frac{dP_l^m(\zeta)}{d\zeta} \right|_{\zeta=\sqrt{1+z^2}}, \quad (18)$$

$$D_{lm}^{EM} = -D_{lm}^{ME} = \sqrt{\frac{4\pi(2l+1)(l-m)!}{l(l+1)(l+m)!}} \frac{im}{z} P_l^m(\sqrt{1+z^2}), \quad (19)$$

where P_l^m is the associated Legendre polynomial of order l . The size of R_m is infinite; therefore, we must truncate the matrix by introducing an upper bound for l , which is denoted by l_{\max} . The accuracy of the Casimir energy is improved by increasing l_{\max} .

Because the factor $\exp(-2d\kappa\sqrt{1+z^2})$ is included in Eq. (17), the main contribution to the Casimir energy at large separations is from small wave numbers $\kappa \sim 1/d$ for fixed z . For small wave numbers, the Mie coefficient $R_{s,1}^E$ dominates all other Mie coefficients. Assuming that the dielectric permittivity of a sphere can be expressed by the

Drude model, $R_{s,1}^E$ at small wave numbers is approximately given by

$$R_{s,1}^E = \frac{2}{3}(\kappa R)^3 + O[(\kappa R)^4]. \quad (20)$$

We further assume that the reflection coefficient of the E mode for small κ and z can be expressed as

$$r_p^E(\kappa, z) = \alpha + \frac{\beta}{\sqrt{1+z^2}}, \quad (21)$$

where parameters α and β are explained in the following sections. The contributions to the Casimir energy at large d for $m = 0$ and 1 are given by

$$E_0(d) = -\frac{\hbar c}{2\pi} \left(\frac{1}{4}\alpha + \frac{3}{32}\beta \right) \frac{1}{d^4}, \quad (22)$$

$$E_1(d) = -2\frac{\hbar c}{2\pi} \left(\frac{3}{16}\alpha + \frac{3}{32}\beta \right) \frac{1}{d^4}. \quad (23)$$

Accordingly, the Casimir energy at asymptotically large separations is given by

$$E_{\text{sp}}^{\text{zero}}(a) \approx -\frac{\hbar c}{2\pi} \left(\frac{5}{8}\alpha + \frac{9}{32}\beta \right) \frac{1}{d^4}, \quad a \gg R. \quad (24)$$

This formulation means that the Casimir energy decays as d^{-4} , and the exponent of the decay is the same as the exponent in the Casimir-Polder formula [23,26]. The Casimir force is given by

$$F_{\text{sp}}(a) = -\frac{dE_{\text{sp}}^{\text{zero}}(a+R)}{da}. \quad (25)$$

Consequently, the Casimir force at large separations is given by

$$F_{\text{sp}}(a) \approx -\frac{\hbar c}{2\pi} \left(\frac{5}{2}\alpha + \frac{9}{8}\beta \right) \frac{1}{(a+R)^5}, \quad a \gg R. \quad (26)$$

Here, we note that the temperature dependence of the Casimir energy cannot be neglected for separations much larger than the sphere's radius [27].

III. LEVITATION NEAR THE INTERFACE BETWEEN LIQUID AND GAS

We consider the levitation of a gold particle in a droplet of bromobenzene, which is enclosed in a vessel as shown in Fig. 2. We assume that the radius of the droplet is sufficiently larger than that of the gold sphere and that the bottom curvature

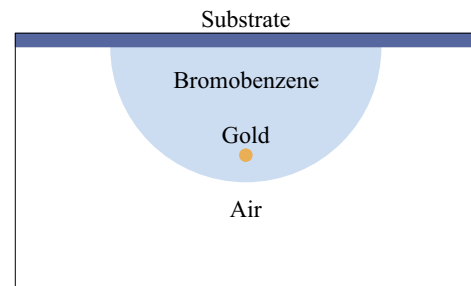


FIG. 2. (Color online) Schematic of a bromobenzene droplet containing a gold sphere. Direction of gravity is perpendicularly downward.

TABLE I. Parameters of the oscillator model for bromobenzene and water taken from Ref. [28].

i	Bromobenzene		Water	
	C_i	ξ_i (eV)	C_i	ξ_i (eV)
1	0.0544	0.00502	1.43	0.0229
2	0.0184	0.0309	9.74	0.000877
3	0.0475	0.111	2.16	0.00493
4	0.532	6.75	0.532	0.103
5	0.645	13.3	0.389	9.50
6	0.24	24.0	0.265	20.9
7	0.00927	99.9	0.136	26.4

of the droplet is zero. Furthermore, the Casimir force between the gold sphere and the substrate is neglected. We use the oscillator model to describe the dielectric permittivity of bromobenzene along the imaginary axis, which is given by Zwol and Palasantzas [28] as follows:

$$\epsilon_3(i\xi) = 1 + \sum_{i=1}^7 \frac{C_i}{1 + (\xi/\omega_i)^2}, \quad (27)$$

where coefficient C_i and resonance frequency ω_i are given in Table I. For gold, we use the Drude model:

$$\epsilon_1(i\xi) = 1 + \frac{\omega_p^2}{\xi(\xi + \gamma)}, \quad (28)$$

where $\omega_p = 9.0$ eV and $\gamma = 0.035$ eV [29]. Figure 3 shows the dielectric permittivity of bromobenzene (dashed line) and gold (dashed-dotted line) along the imaginary axis. The gas surrounding the droplet is a mixture of bromobenzene and air, and its dielectric permittivity is much smaller than that of liquid bromobenzene. Thus, we assume that the dielectric permittivity is 1 for any frequency.

Figure 4 shows the Casimir force $F(a)$ acting on gold spheres of $R = 100$ and 500 nm in a log-log scale. The thick solid line shows the value obtained using the scattering-matrix formulation with $l_{\max} = 25$. To estimate error $\Delta(a)$ in the Casimir force, the difference between the values of the Casimir force calculated with $l_{\max} = 25$ and with $l_{\max} = 20$, which is

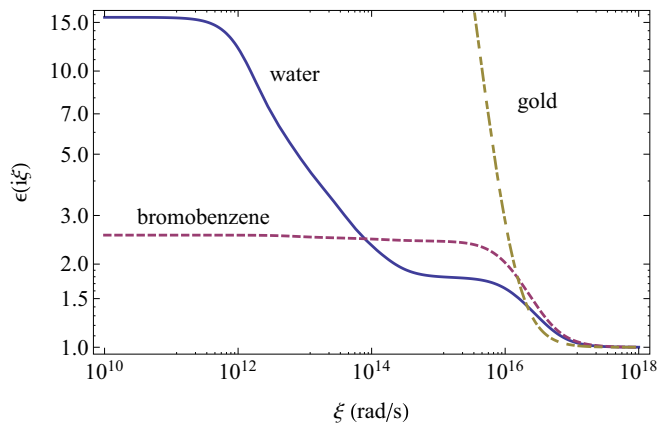


FIG. 3. (Color online) Dielectric permittivity of bromobenzene, water, and gold along the imaginary frequency axis.

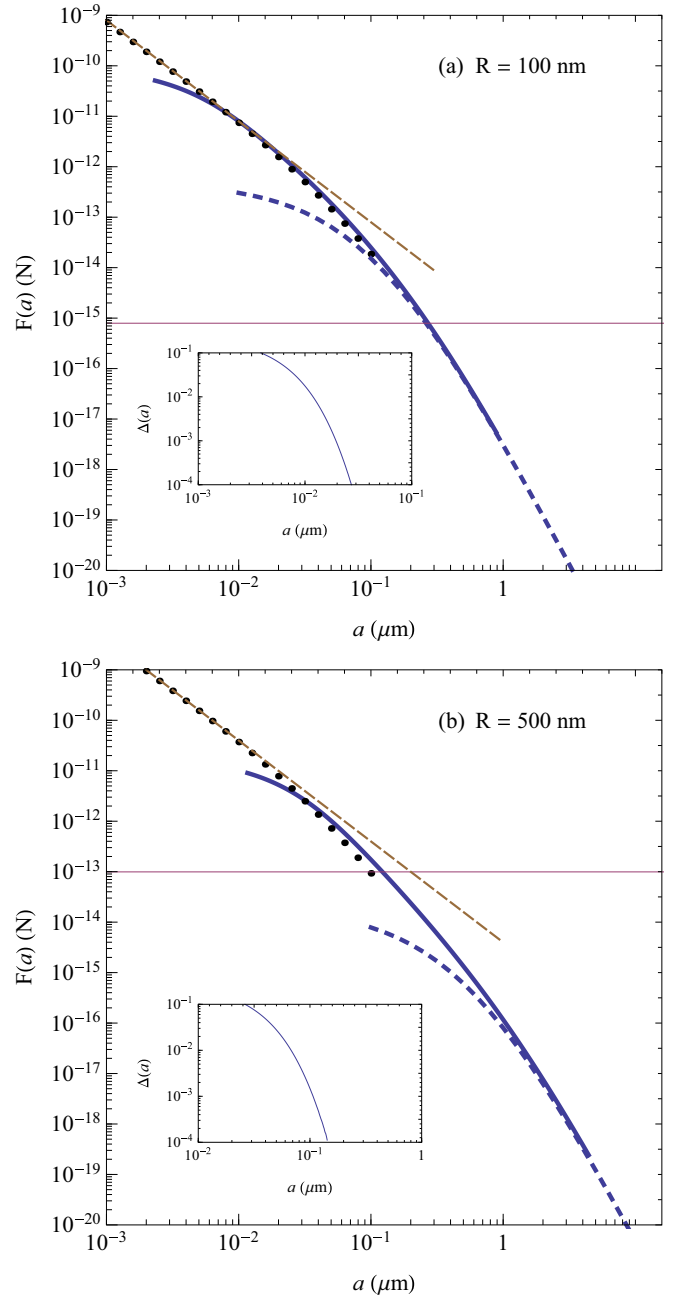


FIG. 4. (Color online) Casimir force acting on a gold sphere near a bromobenzene-air interface for (a) $R = 100$ nm and (b) $R = 500$ nm. The thick solid line is calculated using the scattering-matrix formulation. The solid circles show PFA values. The asymptotic Casimir force for small and large separations is shown as thin-long- and thick-short-dashed lines, respectively. The horizontal line represents gravity acting on the gold sphere. The inset shows the relative difference between the Casimir forces with $l_{\max} = 25$ and 20.

normalized by the Casimir force with $l_{\max} = 25$, is shown in the inset. The error becomes small as the separation increases. The asymptotic behavior for small and large separations is shown using thin, long- and thick, short-dashed lines, respectively.

For large separations, the contribution near $\kappa = 0$ is significant, and the reflection coefficient $r_p(\kappa, z)$ near $\kappa = 0$ can be approximated as $\alpha + \beta/\sqrt{1+z^2}$ near $z = 0$; this result is identical to Eq. (21) if the dielectric permittivity is expressed using the oscillation model. The values α and β defined in Eq. (21) are determined by the reflection coefficient of the plate near zero frequency:

$$\beta = - \left. \frac{d^2 r_p^E(0, z)}{dz^2} \right|_{z=0}, \quad (29)$$

$$\alpha = r_p^E(0, 0) - \beta. \quad (30)$$

As separation increases, the Casimir force given by the scattering-matrix formulation asymptotically approaches the value given by Eq. (26), which is shown by the thick-short-dashed line in Fig. 4. Conversely, at small separations, the solid circles, which show the values obtained using the PFA at 300 K, asymptotically approach the thin-long-dashed line, which shows values calculated from Eq. (8). These results show that the Casimir force acting on a gold sphere in a bromobenzene droplet is repulsive across the entire range of separations. In addition, we find that the Casimir force at room temperature can be well approximated by the Casimir force at absolute zero for small separations.

The horizontal line indicates the gravitational force acting on the sphere. We define the levitation distance as the height at which the repulsive Casimir force balances the resultant of gravity and buoyancy. Using the mass densities of bromobenzene 1.489 g/cm^3 [30] and gold 19.32 g/cm^3 , the separation distances obtained from the scattering-matrix formulation are 271 and 122 nm for $R = 100$ and 500 nm, respectively. Error $\Delta(a)$ in the Casimir force near the equilibrium position is large for $R = 500$ nm; the accuracy of the levitation height for larger spheres is relatively less accurate.

IV. LEVITATION NEAR THE INTERFACE BETWEEN LIQUID AND LIQUID

A. The direction of the Casimir force and the levitation height

The strength of the repulsive Casimir force increases as ϵ_2 decreases, when the condition $\epsilon_2(i\xi) < \epsilon_3(i\xi) < \epsilon_1(i\xi)$ is satisfied. The dielectric permittivity along the imaginary axis is always greater than 1. Therefore, the repulsive Casimir force near an interface between a liquid and air, for which the dielectric permittivity is almost 1 at any frequency, can be large in comparison with the dielectric permittivity near other interfaces. However, because of convection and evaporation, the interface between a liquid and gas often becomes unstable. In this section, we consider the levitation of a gold sphere near a bromobenzene-water interface because a liquid-liquid interface is more stable than a gas-liquid interface. The schematic of the bromobenzene-water interface considered in this study is illustrated by interchanging air with water in Fig. 2.

The dielectric permittivity of water along the imaginary axis is also expressed by the oscillator model, and the parameters are given in Table I. At low frequencies, the dielectric permittivity of water is larger than that of bromobenzene. Therefore, the inequality $\epsilon_2(i\xi) < \epsilon_3(i\xi) < \epsilon_1(i\xi)$ is not satisfied for

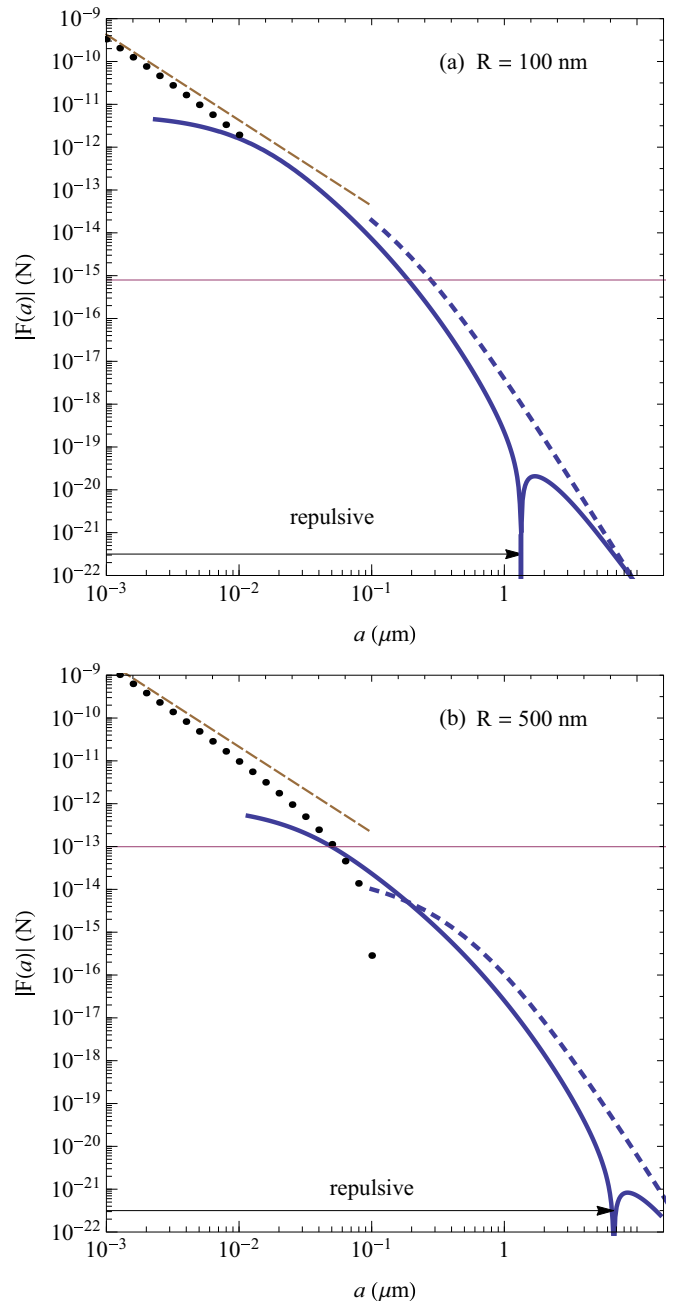


FIG. 5. (Color online) Casimir force acting on a gold sphere near a bromobenzene-water interface for (a) $R = 100$ nm and (b) 500 nm. The thick solid line is calculated using the scattering-matrix formulation. The solid circles show PFA values. The asymptotic Casimir force at small and large separations is shown as thin-long- and thick-short-dashed lines, respectively. The horizontal line represents gravity acting on the gold sphere.

small ξ . Figure 5 shows the absolute value of the Casimir force acting on gold spheres with radii $R = 100$ and 500 nm in a log-log scale. The direction of the Casimir force shows that, for $R = 100$ nm, this force is repulsive below $a = 1.3 \mu\text{m}$ and becomes attractive above $1.3 \mu\text{m}$. This change results from the reversal of the dielectric permittivity's order. As shown in Sec. II, the asymptotic behavior of the Casimir force for large separations is determined by the dielectric permittivity near

zero frequency. The static dielectric permittivity of water is larger than that of bromobenzene. Accordingly, the Casimir force is attractive for large separations, and the absolute value of the Casimir force decays proportionally as d^{-5} . The thick-short-dashed line shows the absolute value of the Casimir force for large separations, as given by Eq. (26). The levitation height of the 100-nm gold sphere near the interface between bromobenzene and water is 188 nm, which is less than the height obtained near the bromobenzene-air interface. The levitation height for the 500-nm sphere could not be calculated because of the low convergence of the scattering-matrix formulation.

We assumed that the dielectric permittivity changes discontinuously across the interface between bromobenzene and water. Bromobenzene is a nonpolar molecule, while water is a polar molecule. Therefore, bromobenzene is mostly insoluble in water. However, bromobenzene and water undergo slight mixing near the interface. Although we cannot show the change in the densities of bromobenzene and water across their interface, the transition width is presumably less than 1 nm because Linse reported that the intrinsic interface between benzene and water is molecularly sharp by using Monte Carlo simulation [31]. Therefore, the error in the levitation height resulting from the mixing of molecules is likely small. Surface roughness correction is usually necessary for measuring the Casimir force above a solid surface. However, it is likely that the liquid-liquid interface is smoother than solid surfaces.

B. Dielectrophoresis force and surface tension

Thus far, we have considered levitation without considering the electrostatic force acting on the gold sphere. Arising from the contact potential difference between different materials, the electrostatic force has often affected previous measurements of the Casimir force [32]. However, the levitated gold particle is electrically disconnected from the substrate, and its effect on levitation is presumably small. Alternatively, the electrostatic force can possibly be generated by the surface potential, which arises from the broken symmetry in the spatial charge distribution near the interface. To our knowledge, previous studies have not investigated the surface potential between bromobenzene and water; therefore we attempt to estimate the electrostatic force acting on a gold sphere using the surface potential at the interface between water and vapor. Kathmann *et al.* computed the *ab initio* surface potential of water $\phi(z)$ [33,34] and fitted its spatial dependence using a hyperbolic tangent, as shown in Fig. 6, in which the origin of the z axis is located at the Gibbs dividing surface [35]. The computed surface potential of water is 3.1 V, and this potential is larger than typical values of the contact potential, which are on the order of tens of millivolts. However, the electrostatic force does not directly depend on the surface potential. A dielectric sphere is not influenced by the electrostatic force if the dielectric sphere is located in a uniform electric field. When a dielectric sphere including a metallic sphere as a special case is located in a nonuniform electric field, the dielectrophoresis force acts on the dielectric sphere. The dielectrophoresis force [36] acting on a neutral metallic sphere of radius R surrounded by a medium with relative dielectric constant ϵ_m is

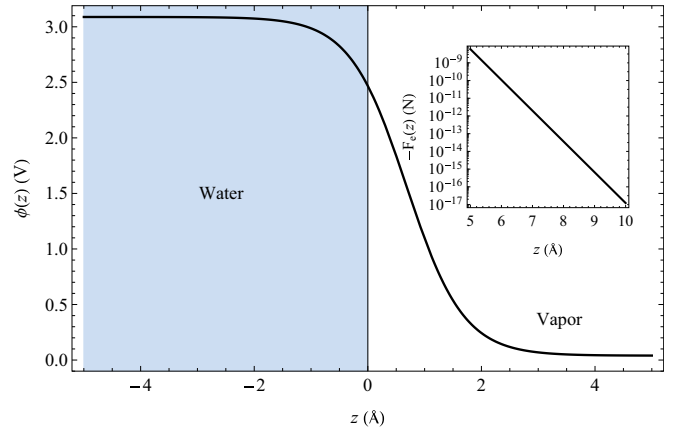


FIG. 6. (Color online) Surface potential for the interface between water and vapor, taken from Ref. [33]. The origin of z is located at the Gibbs dividing surface. Inset is the dielectrophoresis force acting on a gold sphere of radius 100 nm at z .

given by

$$F_e(z) = 2\pi R\epsilon_m\epsilon_0 \frac{d}{dz} \left(\frac{d\phi(z)}{dz} \right)^2, \quad (31)$$

where ϵ_0 denotes the dielectric permittivity of vacuum. The inset of Fig. 6 shows the dielectrophoresis force acting on a gold sphere of radius 100 nm in bromobenzene, for which the relative dielectric constant is 5.3 [3,16]. We assumed that the surface potential for the bromobenzene-water interface can be approximated by the surface potential for the water-vapor interface. With respect to the position, the differential coefficient of the surface potential decreases very rapidly as the distance increases. Therefore, the dielectrophoresis force has little effect on the levitated particle if the levitation height is much larger than about 1 nm.

We have assumed that the gold sphere is neutral. If a gold sphere is charged, Eq. (31) must be modified [37]. However, the change in the dielectrophoresis force arising from this modification is minor, and the additional electrostatic force acting on a charged particle with the surface charge density σ is given by $-4\pi R^2\sigma\phi'(z)$. Using the surface potential obtained by Kathmann *et al.*, $\phi(z) = 1.52434 \tanh(z + 0.68177 \text{ \AA}) + 1.56409 \text{ V}$ [35], the strength of the electrostatic force acting on a sphere with a 100-nm radius at z (in unit of Ångstrom) is estimated to be $1.9 \times 10^{-3} \sigma e^{-2z} \text{ N}$ for large z . We recall that the levitation height of a 100-nm gold sphere is 188 nm near the bromobenzene-water interface and find that, compared with the Casimir force, the electrostatic force at the separation is very small. If both the gold sphere and the bromobenzene-water interface are charged, a stronger electrostatic force may act on the gold sphere. We assume that the surface charge density at the bromobenzene-water interface is identical to the surface charge density of a gold sphere but has the opposite sign. Consequently, the electrostatic force is approximately given by $-4\pi R^2\sigma^2/2\epsilon_m\epsilon_0$, and we estimate that the surface charge density necessary to cancel the levitation force is $7.7 \times 10^{-7} \text{ C/m}^2$. This value is about 0.13% of the surface charge density (0.01 C/m²) of a charged-stabilized gold nanoparticle made by the method of Frens [38,39]. The residual charge

must be removed to demonstrate levitation resulting from the repulsive Casimir force, and the conclusion may be verified by applying an external electric field [40].

We consider the stability of levitation produced by the repulsive Casimir force. If a gold sphere approaches the interface because of Brownian motion, the dielectrophoresis force, which is larger than the Casimir force, attracts the gold sphere toward the interface. If the separation distance is zero, the difference between the potential at the interface and that at infinity is expressed by

$$\Delta E = -\pi R^2 \gamma_{32} \left[1 - \frac{\gamma_{12} - \gamma_{13}}{\gamma_{32}} \right]^2, \quad (32)$$

where γ_{32} , γ_{13} , and γ_{12} are the surface tension values of the bromobenzene-water, gold-bromobenzene, and gold-water interfaces, respectively [41,42]. This equation is often used to consider nanoparticle assemblies at liquid-liquid interfaces. Lin *et al.* showed that ΔE is about $-5k_B T$ for cadmium selenide (CdSe) covered by tri-*n*-octylphosphine oxide with a 2.8 nm radius at the toluene-water interface using $\gamma_{32} = 35.7$ mN/m, $\gamma_{13} \sim 15$ mN/m, and $\gamma_{12} \sim 40$ mN/m. Here, γ_{32} , γ_{13} , and γ_{12} are the surface tension values of toluene-water, CdSe-toluene, and CdSe-water interfaces, respectively. We could not calculate the potential drop at the bromobenzene-water interface because of the lack of experimental data. However, we conjecture that a gold particle with a radius larger than 100 nm is stable at the bromobenzene-water interface. The interfacial tension of the bromobenzene-water interface is 31.2 mN/m [43]. If $\gamma_{12} = \gamma_{13}$, the potential drops to a minimum value of $-\pi R^2 \gamma_{32}$, which yields a large potential drop of $2.4 \times 10^5 k_B T$ for a 100-nm gold sphere. Conversely, to satisfy $|\Delta E| < k_B T$, the difference between γ_{12} and γ_{13} must be equal to γ_{32} within an error of 2%, and it is unlikely that this situation would be realized. Therefore, if a gold sphere is trapped at the interface between bromobenzene and water, escape from the interface is unlikely.

V. CONCLUSIONS

We have examined the possibility of levitating a particle using the repulsive Casimir force near both a gas-liquid and liquid-liquid interface. First, we showed that the Casimir force acting on a gold sphere near a bromobenzene-air interface is always repulsive. Compared with the dielectric permittivity of a liquid, the dielectric permittivity of a gas along the imaginary axis is small. The Casimir energy decreases when the volume of the liquid between the gold sphere and the interface increases, and therefore the gold sphere separates from the interface. The estimated levitation height of the 100-nm gold sphere in a bromobenzene droplet is larger than 200 nm, which is twice the radius. This conclusion

means that at equilibrium, the PFA is not valid, and the scattering-matrix formulation is more suitable for calculating the Casimir force. We can directly observe gold particles with radii of several hundred nanometers in a liquid droplet using dark field microscopy. However, because of convection, the gold particle may move within a liquid, and equipment that suppresses convection is required to verify that the levitation is indeed caused by the repulsive Casimir force.

Secondly, we have shown that a gold sphere can also be levitated by the repulsive Casimir force near a bromobenzene-water interface. Compared to an organic liquid, water has a large static dielectric permittivity. This seems unsuitable for generating the repulsive Casimir force inside bromobenzene near the bromobenzene-water interface. However, the dielectric permittivity of water decreases more rapidly than that of an organic liquid along the imaginary frequency. Therefore, at higher imaginary frequencies, the liquid-liquid interface is similar to the gas-liquid interface in terms of the dielectric permittivity. This change in the dielectric permittivity results in a change in the direction of the Casimir force. For small separations, the Casimir force is repulsive; however, the force becomes attractive as the separation between the gold sphere and the interface increases. This finding means that the Casimir force vanishes at a finite separation distance, at which the sphere's location is stable.

Unlike a gas-liquid interface, a liquid-liquid interface is more stable because the liquid does not evaporate and convection is suppressed. We considered the levitation of a gold particle in a bromobenzene droplet, and for simplicity, its curvature was assumed to be zero. The advantage of levitation in a droplet with a positive curvature is that a single gold particle can be trapped at the bottom of the droplet. However, this trap may be metastable because the position at the interface is more stable. The escape rate from the equilibrium position, where the sum of the Casimir force, gravity, and buoyancy is zero, depends on both the potential barrier formed by the Casimir effect and the electric field caused by dipole moments of water. Unlike previous studies, which were largely based on surface tension, this study focuses on the stability of nanoparticles near a liquid-liquid interface by considering the Casimir force. New calculation methods for the Casimir force will provide further insights into the dynamics of nanoparticles near interfaces.

ACKNOWLEDGMENTS

This research was supported by the Ministry of Education, Culture, Sports, Science and Technology, Grant-in-Aid for Scientific Research(C), MEXT KAKENHI Grant No. 13240323, and Sanyo Special Steel Cultural Promotion Foundation.

[1] M. Bordag, G. L. Klimchitskaya, U. Mohideen, and V. M. Mostepanenko, *Advances in the Casimir Effect* (Oxford University Press, New York, 2009).

[2] D. Dalvit, P. Milonni, D. Roberts, and F. Rosa, *Casimir Physics* (Springer-Verlag, Heidelberg, 2011).

[3] A. Milling, P. Mulvaney, and I. Larson, *J. Colloid Interface Sci.* **180**, 460 (1996).

- [4] O. Kenneth, I. Klich, A. Mann, and M. Revzen, *Phys. Rev. Lett.* **89**, 033001 (2002).
- [5] S. A. Fulling, L. Kaplan, and J. H. Wilson, *Phys. Rev. A* **76**, 012118 (2007).
- [6] I. G. Pirozhenko and A. Lambrecht, *J. Phys. A* **41**, 164015 (2008).
- [7] F. S. S. Rosa, D. A. R. Dalvit, and P. W. Milonni, *Phys. Rev. Lett.* **100**, 183602 (2008).
- [8] A. W. Rodriguez, J. D. Joannopoulos, and S. G. Johnson, *Phys. Rev. A* **77**, 062107 (2008).
- [9] V. Yannopoulos and N. V. Vitanov, *Phys. Rev. Lett.* **103**, 120401 (2009).
- [10] R. Zhao, J. Zhou, Th. Koschny, E. N. Economou, and C. M. Soukoulis, *Phys. Rev. Lett.* **103**, 103602 (2009).
- [11] A. Azari, M. F. Miri, and R. Golestanian, *Phys. Rev. A* **82**, 032512 (2010).
- [12] M. Levin, A. P. McCauley, A. W. Rodriguez, M. T. Homer Reid, and S. G. Johnson, *Phys. Rev. Lett.* **105**, 090403 (2010).
- [13] A. G. Grushin and A. Cortijo, *Phys. Rev. Lett.* **106**, 020403 (2011).
- [14] N. Inui, *Phys. Rev. A* **86**, 022520 (2012).
- [15] N. Inui, *J. Appl. Phys.* **111**, 074304 (2012).
- [16] J. N. Munday, F. Capasso, and V. A. Parsegian, *Nature (London)* **457**, 170 (2009).
- [17] M. Ishikawa, N. Inui, M. Ichikawa, and K. Miura, *J. Phys. Soc. Jpn.* **80**, 114601 (2011).
- [18] F. Capasso, J. N. Munday, and Ho Bun Chan, in *Casimir Physics*, edited by D. Dalvit, P. Milonni, D. Roberts, and F. Rosa (Springer-Verlag, Heidelberg, 2011).
- [19] N. Inui and K. Goto, *Phys. Rev. E* **88**, 052133 (2013).
- [20] T. Emig, N. Graham, R. L. Jaffe, and M. Kardar, *Phys. Rev. Lett.* **99**, 170403 (2007).
- [21] P. A. Maia Neto, A. Lambrecht, and S. Reynaud, *Phys. Rev. A* **78**, 012115 (2008).
- [22] R. Zandi, T. Emig, and U. Mohideen, *Phys. Rev. B* **81**, 195423 (2010).
- [23] A. Canaguier-Durand, A. Gerardin, R. Guerout, P. A. Maia Neto, V. V. Nesvizhevsky, A. Y. Voronin, A. Lambrecht, and S. Reynaud, *Phys. Rev. A* **83**, 032508 (2011).
- [24] C. Hertlein, L. Helden, A. Gambassi, S. Dietrich, and C. Bechinger, *Nature(London)* **451**, 172 (2008).
- [25] E. M. Lifshitz, *Sov. Phys. JETP* **2**, 73 (1956).
- [26] H. B. G. Casimir and D. Polder, *Phys. Rev.* **73**, 360 (1948).
- [27] A. O. Sushkov, W. J. Kim, D. A. R. Dalvit, and S. K. Lamoreaux, *Nat. Phys.* **7**, 230 (2011).
- [28] P. J. van Zwol and G. Palasantzas, *Phys. Rev. A* **81**, 062502 (2010).
- [29] A. Lambrecht and S. Reynaud, *Eur. Phys. J. D* **8**, 309 (2000).
- [30] J. N. Nayak, M. I. Aralaguppi, and T. M. Aminabhavi, *J. Chem. Eng. Data* **48**, 628 (2003).
- [31] P. Linse, *J. Chem. Phys.* **86**, 4177 (1987).
- [32] U. Mohideen and A. Roy, *Phys. Rev. Lett.* **81**, 4549 (1998).
- [33] S. M. Kathmann, I. W. Kuo, C. J. Mundy, and G. K. Schenter, *J. Phys. Chem. B* **115**, 4369 (2011).
- [34] K. Leung, *Phys. Chem. Lett.* **1**, 496 (2010).
- [35] S. M. Kathmann, I. W. Kuo, and C. J. Mundy, *J. Am. Chem. Soc.* **131**, 17522 (2009).
- [36] H. A. Pohl, *J. Appl. Phys.* **29**, 1182 (1958).
- [37] J. P. Huang, M. Karttunen, K. W. Yu, and L. Dong, *Phys. Rev. E* **67**, 021403 (2003).
- [38] F. Reincke, S. G. Hickey, W. K. Kegel, and D. Vanmaekelbergh, *Angew. Chem., Int. Ed.* **43**, 458 (2004).
- [39] G. Frens, *Nat. Phys. Sci.* **241**, 20 (1973).
- [40] M. N. Martin, J. I. Basham, P. Chando, and S-K. Eah, *Langmuir* **26**, 7410 (2010).
- [41] Y. Lin, H. Skaff, T. Emrick, A. D. Dinsmore, and T. P. Russel, *Science* **299**, 5604 (2003).
- [42] P. Pieranski, *Phys. Rev. Lett.* **45**, 569 (1980).
- [43] A. H. Demond and A. S. Lindner, *Environ. Sci. Technol.* **27**, 2318 (1993).